Effects of the Polarizability and Packing Density of Transparent Oxide Films on Water Vapor Permeation

Won Hoe Koo, Soon Moon Jeong, Sang Hun Choi, Woo Jin Kim, and Hong Koo Baik*

Department of Metallurgical Engineering, Yonsei University, Seoul 120-749, Korea

Sung Man Lee

Department of Advanced Material Science and Engineering, Kangwon National University ChunCheon, Kangwon-do 200-701, Korea

Se Jong Lee

Department of Materials Engineering, Kyungsung University, Busan, 608-736, Korea

Received: March 2, 2005; In Final Form: April 18, 2005

The tin oxide and silicon oxide films have been deposited on polycarbonate substrates as gas barrier films, using a thermal evaporation and ion beam assisted deposition process. The oxide films deposited by ion beam assisted deposition show a much lower water vapor transmission rate than those by thermal evaporation. The tin oxide films show a similar water vapor transmission rate to the silicon oxide films in thermal evaporation but a lower water vapor transmission rate in IBAD. These results are related to the fact that the permeation of water vapor with a large dipole moment is affected by the chemistry of oxides and the packing density of the oxide films. The permeation mechanism of water vapor through the oxide films is discussed in terms of the chemical interaction with water vapor and the microstructure of the oxide films. The chemical interaction of water vapor with oxide films has been investigated by the refractive index from ellipsometry and the OH group peak from X-ray photoelectron spectroscopy, and the microstructure of the composite oxide films was characterized using atomic force microscopy and a transmission electron microscope. The activation energy for water vapor permeation through the oxide films has also been measured in relation to the permeation mechanism of water vapor. The diffusivity of water vapor for the tin oxide films has been calculated from the time lag plot, and its implications are discussed.

1. Introduction

Inorganic transparent oxide films such as silicon- and aluminum-oxide on polymer substrates have been widely used as a gas barrier in the fields of food packaging, medical devices, and, recently, flexible display industries. Especially, for passivation of organic light emitting devices (OLEDs) requiring extremely low water vapor transmission rate (WVTR) of $<10^{-6}$ g/m^2/day at 100% RH and 25 °C,[1] relatively dense oxynitride films such as AlO_xN_y and SiO_xN_y, compared to AlO_x and SiO_x, have been studied as transparent gas barrier materials using sputtering and plasma enhanced chemical vapor deposition (PECVD).[2−4] However, since these reported barrier films show too high WVTR to be applied to display industries and the permeation mechanism of water vapor is not well-known, a new barrier material design based on the permeation mechanism of water vapor is required to perfectly protect the permeation of water vapor. Also, because all layers except for indium tin oxide in OLEDs are deposited by thermal evaporation, it is profitable that a new barrier material can be deposited by thermal evaporation for a continuous process.

Water with a large dipole moment chemically interacts with the oxides, and thus, the water transmission rate can be affected by the chemistry of oxides.[5] In a previous paper, we reported that, in the transparent SnO_2-SiO_x composite films deposited by thermal evaporation, the polarizability expressed as refractive index and packing density of the films plays an important role on the permeation of water vapor through oxide films, and thus, the 80% SnO_2 films showing the highest polarizability and packing density have the lowest WVTR.[6] Nevertheless, the WVTR is too high to be used as a passivation layer in OLEDs, because the thin films deposited by thermal evaporation generally show the low packing density with the loose microstructure due to low adatom mobility.

In this study, we controlled the packing density of the SnO_2 films with high polarizability and the SiO_x films with low polarizability, using ion beam assisted deposition (IBAD) for a better water barrier performance, and investigated the effect of the packing density and the polarizability of the oxide films on the permeation of water vapor, in terms of the microstructure and chemical interaction with water vapor of the oxide films.

2. Experimental Section

The SiO_x and SnO_2 films were deposited on optical grade polycarbonates (PC), Si(100) wafer, and silica glass substrates by thermal evaporation and also by the IBAD process, using an End-Hall ion gun. The PC substrates with the thickness of 200 μm have no "antiblock" particle inducing microscale defects in the deposited films and very smooth surface of the rms

* Corresponding author. Fax: +82-2-312-5375. E-mail: thinfilm@yonsei.ac.kr.

10.1021/jp051051r CCC: $30.25
Published on Web 05/17/2005

(surface roughness) below 1 nm. An antielectrostatic gun was used to remove the surface electrostatic charge on the PC substrates following the cleaning with alcohol. The working pressure was kept at 1.1×10^{-2} Pa with a flow rate of oxygen of 2 sccm in thermal evaporation method and at 2.67×10^{-2} Pa with a flow rate of oxygen of 1.5 sccm and argon of 3 sccm in the IBAD process. The anode voltage of the End-Hall ion gun was set to 150 V, and the ion beam current incident on the substrate measured by a Faraday cup varied from 10 to 45 μA/cm^2 to control the packing density of the films, because the End-Hall ion gun is generally used for low ion beam energy below 200 eV and high ion beam current. The evaporation source materials were the powders of SiO and SnO_2 with purities of 99.99% and 99.9%, respectively. The film growth rate was maintained at 0.1 nm/s by using a quartz crystal monitor and the films thickness was fixed at 80 nm.

The optical transmittance and reflectance of the films deposited on glass substrates were recorded in the wavelength ranges of 250−800 nm by a spectrophotometer (Shimadzu UV-3101PC). An Al-coated reflector was used as a reference for the reflectance. The refractive index for the thin films deposited on the Si(100) substrates was measured at 633 nm by a L117 ellipsometer (Gaertner Scientific Corporation). The structure of the deposited films on the PC substrates was determined by XRD (Rigaku, D/max-RINT 2700) operating at 30 kV, 20 mA, using a Cu Kα1 line ($\lambda = 0.154056$ nm), and all of the films showed the amorphous structure. The surface morphology of the films on the PC substrates was examined by AFM with a Digital Instruments Nanoscope II. The AFM images of 1×1 μm were obtained in tapping mode at a scan rate of 1 Hz, using Si tips with a tip radius of ~10 nm. The microstructure of the SnO_2 films was observed by TEM (JEOL 2010F) operating at 200 keV. For a TEM analysis, the SnO_2 films on PC were placed on 400-mesh copper grids, and the PC substrates were completely dissolved by the heated *o*-chlorophenol vapor to 120 °C. The chemical compositions and the chemical bonding states of the films were analyzed by monochromatic XPS (VG Scientific, ESCARLAB 220-IXL) using an Al Kα X-ray with energy 1486.6 eV and the takeoff angle of 90°. Narrow scan spectra of all regions of interest were recorded with 20 eV pass energy and the binding energy scale was referred to the C1s peak of the carbon contaminating the sample surface at a value of 284.6 eV. The water vapor transmission rate (WVTR) and activation energy for water vapor permeation were measured at 100% relative humidity (RH) using a Permatran W 3/31 (Modern Controls, Inc.). The samples were masked with aluminum foil having a 5 cm^2 gas exposure area for water vapor transmission, and the data were taken at the temperatures ranging from 27 to 47.8 °C. For calculating the diffusivity for the SnO_2 films deposited on the PC by IBAD, the samples were dried in a vacuum at around 80 °C.

3. Results and Discussion

3.1. Chemical Composition and Optical Properties. The composition and chemical states of the deposited films by thermal evaporation and IBAD were analyzed by XPS. From the Si2p and Sn3d peak deconvolution, we found that the SiO_x films and the SnO_x films by thermal evaporation have oxygen compositions of 1.7 and 1.95, respectively, and all films by IBAD have oxygen compositions of 1.91 and 2.02, respectively.

Variations of the refractive index of the SiO_x and SnO_2 films by thermal evaporation and IBAD at the ion beam current density of 45 μA/cm^2 are presented in Figure 1a. The SiO_x and SnO_2 films by thermal evaporation show the refractive index

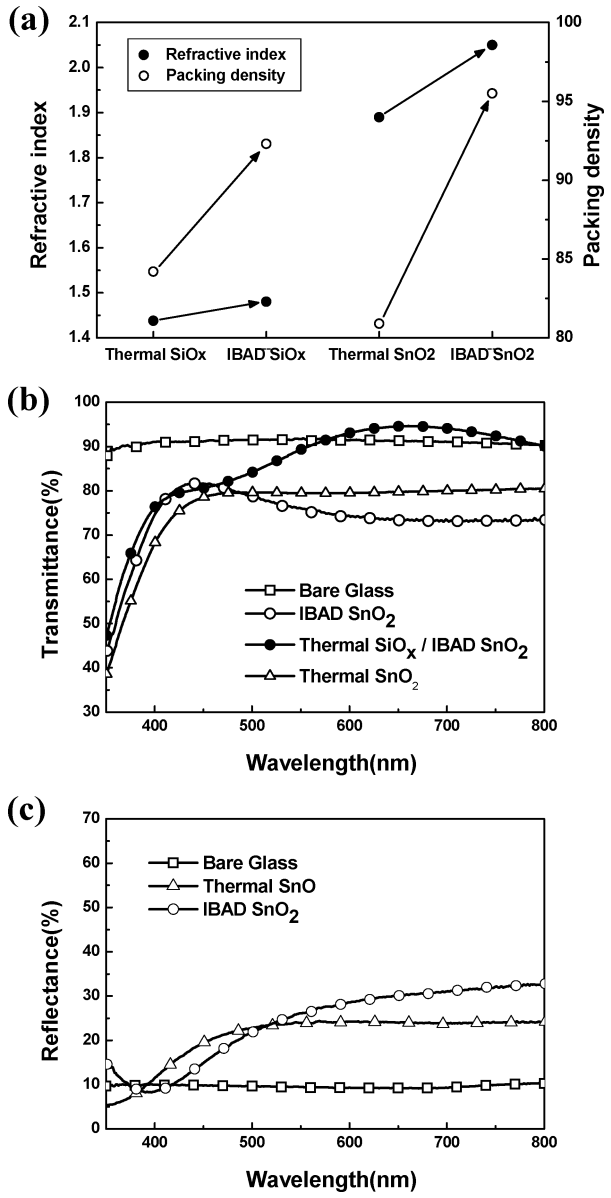

Figure 1. (a) The refractive index (left axis) and the packing density (right axis) of the SiO_x films and SnO_2 films by thermal evaporation and IBAD at the ion current density of 45 μA/cm^2. (b) The optical transmittance of the SnO_2 films by thermal evaporation and IBAD at the ion current density of 45 μA/cm^2, and of the multilayer consisting of IBAD SnO_2(80 nm)/thermal SiO_x(100 nm)/glass. (c) The optical reflectance of the SnO_2 films by thermal evaporation and IBAD at the ion current density of 45 μA/cm^2.

of 1.44 and 1.89, respectively. Since ion bombardment during deposition in IBAD promotes film densification and the film densification is closely related to the refractive index, resulting in the increase of the refractive index, the SiO_x and SnO_2 films by IBAD show the increased refractive index values of 1.48 and 2.05, respectively.

The high refractive index of the SnO_2 films decreases the optical transmittance because of the increased reflectance due to the optical interference with the silica substrate with the refractive index of around 1.52. Although the SnO_2 films by thermal evaporation show a transmittance of around 80%, the SnO_2 films by IBAD show tahe lower transmittance of around 75%, because of the increased reflectance due to the higher refractive index, as seen in Figure 1, panels b and c. Since the proper optical design using the films of the high and low refractive index minimizes the reflectance, the multilayer

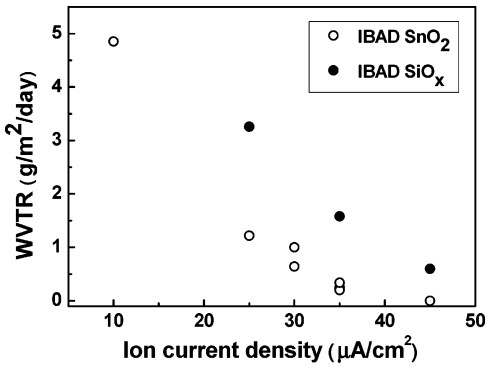

Figure 2. (a) Water vapor transmission rate (WVTR) of the SiO_x films (●) and SnO_2 films (○) deposited by IBAD process as a function of the ion current density, measured at 37.8 °C and 100% RH.

consisting of IBAD SnO_2(80 nm)/thermal SiO_x(100 nm)/glass in Figure 1b minimizes the reflectance and, thus, shows the transmittance over 90% at around 630 nm, where the refractive index of the films was measured by the ellipsometer. Therefore, the transparent SnO_2 films with the high refractive index by IBAD can be used as optical films to modulate the optical properties such as organic microcavity light emitting diodes,[7] in addition to passivation layers or gas barriers.

3.2. Water Vapor Transmission Rate (WVTR). Figure 2 shows the WVTR of the SiO_x and SnO_2 films deposited by the IBAD process as a function of the ion beam current density, measured at 37.8 °C and 100% RH. The SiO_x and SnO_x films by thermal evaporation without ion beam irradiation have a WVTR of about 14 g/m^2 day, providing approximately 2.4 times the improvement in WVTR, compared to the bare PC substrate (34 g/m^2·day). The poor water vapor barrier properties of the SiO_x films are compared to about 15 times improvement in WVTR of the SiO_x films on PET produced by PECVD[8] and attributed to the loose microstructure due to the low adatom mobility by thermal evaporation. As the ion beam current density increases, the WVTR of the SiO_x and SnO_2 films on the PC substrate rapidly decreases. The ion bombardment during the deposition enhances adatom mobility, decreases the porosity of the deposited films, and thus increases the densification of the films. The SnO_2 films show the lower WVTR than the SiO_x films at all ion beam current densities. At an ion beam current density of 45 μA/cm^2, the SnO_2 films show the WVTR below the measurable limit of 0.01 g/m^2 day, whereas the SiO_x films show a higher WVTR of 0.6 g/m^2 day. The different water barrier properties of the SiO_x films and SnO_2 films at the same ion beam current are originated from the different reactivity with water vapor.

We have investigated the decrease of the WVTR due to the densification of the films by IBAD in aspects of the microstructure of the films and the different water barrier properties of the SiO_x and SnO_2 films in aspects of chemical reactivity with water vapor.

3.2.1. Chemical Effects. Water has a large dipole moment and lone-pair electrons and thus is a good donor. Molecular adsorption occurs by acid/base interaction between water vapor and the oxides. Therefore, strong adsorption on the internal surface of pores and the top surface of oxide films occurs easily in more basic oxides with the generation of the OH group on the surface.[5] Since basicity of oxides, defined as the average electron donor power, is closely related to oxides' polarizability, which can be expressed as the refractive index, oxides with a higher polarizability and refractive index result in the higher OH group density on the top surface and internal surface within pores by stronger interaction with water vapor.[6,9,10] The formed OH groups within pores may interact with permeating water vapor, interrupt the continuous permeation of water vapor, and thus decrease the water vapor transmission rate. The bond strength between OH groups and water bonded to the OH groups is so strong that desorption of water vapor bonded to OH groups begins to occur above 150 °C[11,12] and increases with the polarizability of oxides. Therefore, the higher additional energy is needed for the water vapor permeation through the oxide films with the higher OH group density within pores. In general, the substitution of oxygen by nitrogen in oxides increases the polarizability and refractive index as observed in TiO_xN_y, AlO_xN_y, and SiO_xN_y.[13−15] Erlat et al. reported that the deposited AlO_xN_y films on PET have a lower water vapor transmission rate and higher activation energy than the AlO_x films because of the stronger interaction of water vapor with the AlO_xN_y films.[4]

Figure 3 shows the deconvoluted O1s XPS peaks of the SiO_x and the SnO_2 films by IBAD at the ion beam current density of 45 μA/cm^2. The unsymmetrical O1s peak of the SnO_2 films in Figure 3a shows the peak related to the OH groups at around 531.6 eV with the O1s peak of fwhm 1.23 eV corresponding to the Sn^{4+} at around 530.3 eV. In contrast, the symmetrical O1s peak of the SiO_x films shows no peaks related to the OH groups in Figure 3a except for the O1s peak with fwhm 1.62 eV for SiO_x. Because the polarizability and refractive index of SnO_2 is higher than those of SiO_x, the higher OH group density is formed on the surface and confirmed by the XPS results of Figure 3. Koo et al. reported similar results for the composite films consisting of silicon oxide and tin oxide by thermal evaporation, where the OH group density of the composite films increased with the refractive index.[6]

Therefore, the SnO_2 films with the higher refractive index and the higher OH group density can protect the continuous transfer of water vapor more effectively, and then show the lower WVTR than the SiO_x films at all ion beam current density. However, in the case of thermal evaporation without ion beam irradiation, although the SnO_2 films have a high refractive index of about 1.89, the water vapor transmission rate is similar to the SiO_x films with a refractive index of about 1.44. This is related to the influence of the film porosity on the water vapor permeation, because, if the pore size and density are too large and high, the permeating water vapor would be expected to penetrate the films with little interaction through the central pore space away from the surface OH groups within pores or with weak interaction with the water vapor adsorbed on the surface OH groups within pores.[6] We will discuss the effect of the packing density and microstructure of the SnO_2 films by thermal evaporation and IBAD on the WVTR.

3.2.2. Physical Effects. Generally, the thin films deposited with low adatom mobility at room temperature have an open structure consisting of spherical grains and pores between grains, and the pores act as significant paths for water vapor permeation. The packing density representing the porosity of thin films is closely related to the relative refractive index value of the deposited thin films for the bulk value. By assuming that the pores within the films are accessible to and filled with the molecules of the ambient atmosphere, when the films is exposed to the ambient atmosphere, and thus the refractive index of the pores is 1, the packing density can be simply calculated using the following equation:

$$n_f = pn_s + (1 - p)n_v \quad (1)$$

where p, n_f, n_s, and n_v are the packing density, the index of the film, the index of the solid part of film (that is, grains or

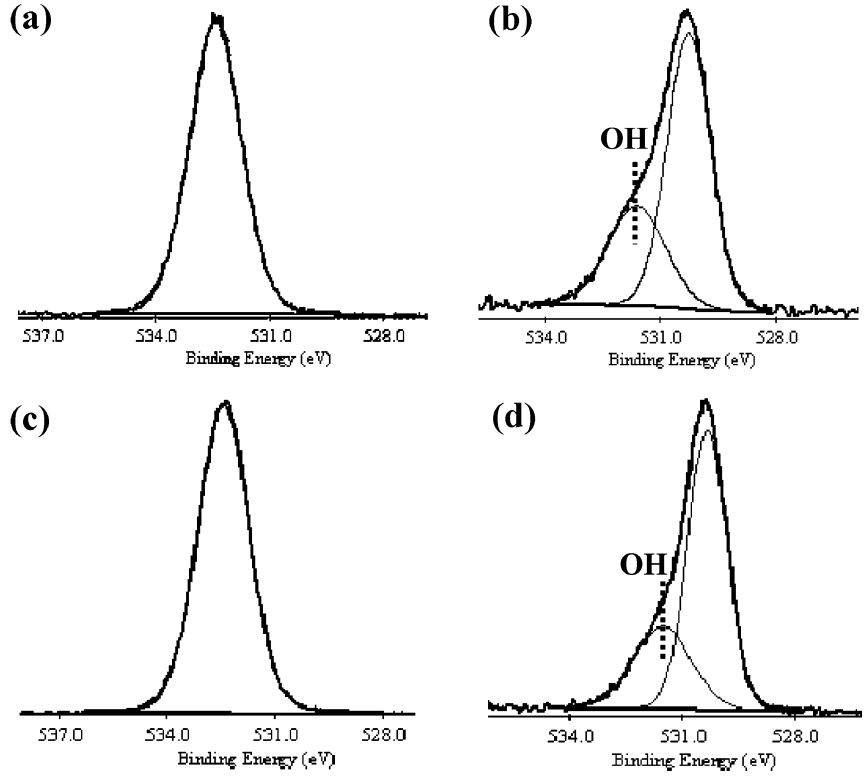

Figure 3. Deconvoluted O1s XPS peaks of the SiO_x films (a) and the SnO_2 films (b) by thermal evaporation, and the SiO_x films (c) and the SnO_2 films (d) by IBAD at the ion current density of 45 μA/cm^2.

columns), and the index of pores in the film, respectively. By applying the refractive index of 1.52 of a bulk silica glass and 2.1 of a bulk SnO_2 for n_s and $n_v = 1$ for air, we can know that the packing density of the SiO_x films and the SnO_2 films by IBAD increased to 92.3% and 95.5% from 84.2% and 80.9% by thermal evaporation, respectively, as presented in Figure 1a. Such a low packing density of the SnO_2 films by thermal evaporation explains the high WVTR similar to the SiO_x films by thermal evaporation, although the SnO_2 films have the higher polarizability.

Figure 4, panels a and b, shows the AFM images of the SnO_2 films by thermal evaporation and IBAD at the ion beam current density of 45 μA/cm^2, respectively. The SnO_2 films in Figure 4a indicate the loose microstructure consisting of large spherical particles with a rms of 2.1 nm, as a result of the low adatom mobility by thermal evaporation. However, in Figure 4b, ion bombardment induces many nucleation sites and enhanced adatom mobility, and thus a densely packed structure composed of fine particles with a rms of 0.7 nm, where the pore size becomes extremely small,[16] in contrast with the large pore size due to a large size of spherical particles. The illustrations and TEM images in Figure 4, panels c and d, reflect on the different microstructures of the SnO_2 films by thermal evaporation and IBAD. The indiscernible contrast in the TEM image of Figure 4d implies that the SnO_2 films by IBAD are composed of densely packed fine particles. However, the SnO_2 films by thermal evaporation show a clear contrast in Figure 4c, due to the loose microstructure consisting of the large particle and pore.[17]

When the pore size of the SnO_2 films with the high refractive index is minimized by ion beam irradiation, the interaction between the permeating water vapor and the OH groups formed on the internal surface within the pores works effectively. Therefore, it is considered that the WVTR for the SnO_2 films deposited at the ion beam current density of 45 μA/cm^2 shows

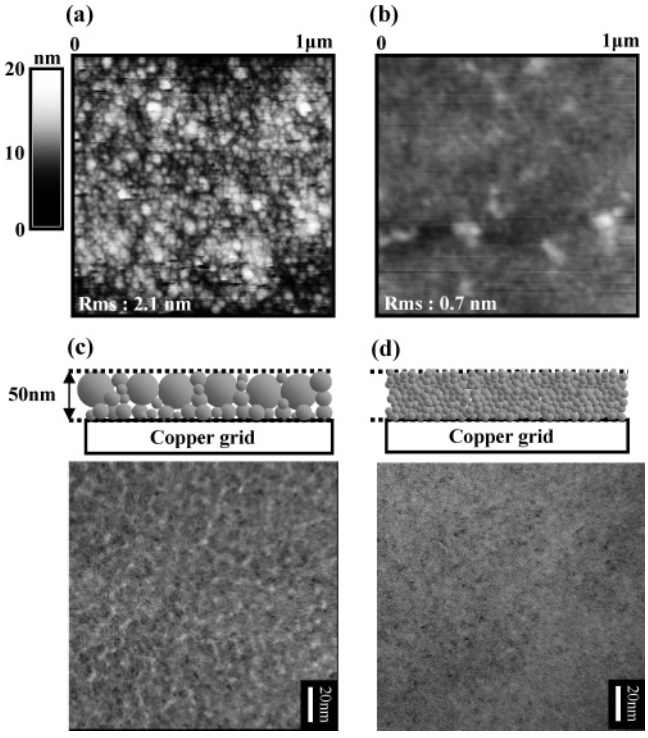

Figure 4. AFM images of the SnO_2 films coated on the PC substrate by thermal evaporation (a) and IBAD (b) at the ion beam current density of 45 μA/cm^2, respectively. The TEM images for each AFM image are also shown in (c) and (d) with the illustrations indicating the microstructure of the SnO_2 films.

the limited value below 0.01 g/m^2 day at 37.8 °C and 100% RH. The degree of the interaction between the permeating water vapor and the formed OH groups, according to the polarizability and pore size of the films can be evaluated by measuring the activation energy for water vapor permeation through the films.

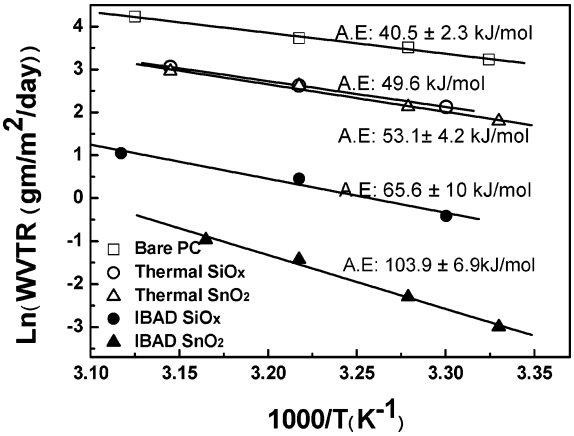

Figure 5. Dependence of WVTR on reciprocal temperature through the bare PC (□), PC/SiO_x films by thermal evaporation (○), PC/SnO_2 films by thermal evaporation (△), PC/SiO_x films by IBAD at the ion current density of 35 μA/cm^2 (●), and PC/SnO_2 films by IBAD at the ion current density of 35 μA/cm^2 (▲). The slope means activation energy for water vapor permeation through the oxide films.

3.3. Activation Energy. The temperature dependence of water vapor transport through the coated polymers below their glass transition temperature can be described by the following Arrhenius equation:

$$\Pi = \Pi_0 \exp(-\Delta E/RT) \tag{2}$$

where Π is the transmission rate, ΔE is the activation energy of permeation, R is the universal gas constant, T is absolute temperature, and Π_0 is a constant unique to the system. Figure 5 shows the water vapor transmission data measured between 27 and 47.8 °C, presented in Arrhenius form with the calculated activation energy from its slope. The SiO_x and SnO_2 film with the WVTR of 1.58 and 0.2 g/m^2 day at the ion beam current density of 35 μA/cm^2 in Figure 2 was used for the activation energy measurement, because the SnO_2 films deposited at the ion beam current density of 45 μA/cm^2 show the WVTR below measurable limit of 0.01 g/m^2 day. The activation energy for water vapor permeation through the thermal-evaporated SiO_x and SnO_2 films is about 9 and 13 kJ/mol higher than that measured for the bare PC (40.5 kcal/mol), respectively. The activation energy of the SiO_x and SnO_2 film by IBAD is about 25 and 63 kJ/mol higher, respectively, compared to that of the bare PC. The increased activation energy for each film implies that the permeating water vapor interacts with the films deposited on the PC, and the different activation energy means that the type and strength of the interaction with water vapor is different according to oxides' polarizability and film porosity.

As we mentioned above, water vapor with a large dipole moment easily adsorbs on the oxide surface, forming the OH groups. Additional water vapor adsorbs on the hydroxylated surface with strong interaction, and then the continuing water vapor adsorbs on top of each other to form mutilayers by weak van der Waals forces of attraction between water vapors. The OH group density and the interaction strength between the OH groups and water vapor are influenced by the polarizability of oxides.[18] In contrast, the water−water interaction is independent of the polarizability of oxides. Raghu et al.[18] measured the desorption energy of water vapor adsorbed on the OH groups and on the adsorbed water vapor, for ZrO_2, HfO_2, and SiO_2 films. The desorption energies of water vapor adsorbed on the OH groups were 33, 27, and 19 kJ/mol, for ZrO_2, HfO_2, and SiO_2 films, respectively, consistent with the order of polarizability. However, the desorption energy of water vapor adsorbed on water vapor was ~13 kJ/mol, similar for all of the oxides and independent of the polarizability of oxides. In the films with a large size of pore and low packing density, the water−water interaction may be dominant during the permeation of water vapor through the films, by the formation of a multilayer of water vapor on the pores. When the pore size is significantly reduced, the interaction between the OH groups and the permeating water vapor may become dominant and thus control the total WVTR through the films on the PC substrates.

The similar activation energy in consideration of the error range and the low additional activation energy in the thermal-evaporated SiO_x and SnO_2 films mean that the water−water interaction independent of the polarizability of the oxides influences the permeation of water vapor through the films. The SiO_x and SnO_2 films deposited at the ion beam current density of 35 μA/cm^2 show the higher activation energy than the thermal-evaporated films, indicating the influence of the interaction between the OH groups and the permeating water vapor. The SnO_2 films show a much higher activation energy of ~104 kJ/mol, whereas the SiO_x films show the activation energy of ~66 kJ/mol. This is because the high OH group density in the SnO_2 films with the significantly reduced pore size by ion bombardment strongly interacts with the permeating water vapor and then protects the permeation of water vapor through the films more effectively. Therefore, such a higher additional energy is needed for the water vapor permeation through the SnO_2 films deposited at the ion beam current density of 35 μA/cm^2, and when the packing density is more enhanced and the pore size is minimized by the increased ion beam current density of 45 μA/cm^2, the SnO_2 films show the WVTR below the measurable limit of 0.01 g/m^2 day.

3.4. Diffusivity. The total WVTR through a bilayer of the film coated on the polymer substrate can be described by a laminate equation such as

$$\frac{1}{J_t} = \frac{1}{J_f} + \frac{1}{J_p} \tag{3}$$

where J_t, J_f, and J_p are the total WVTR, the WVTR of the film, and the WVTR of the polymer substrate, respectively. Since in the case of $J_f \ll J_p$ the WVTR of the polymer substrate can be negligible, the total WVTR through a bilayer is equal to the WVTR through a single layer of the coated film. In a single layer of thickness l and of exposed area A, the concentration profile of water vapor as a function of distance (x) and time (t) is given with the assumptions that (1) the upstream side of the film at $x = 0$ is in contact with 100% RH and saturated at a constant concentration C_0, (2) the downstream side of the films at $x = l$ is swept with a dry gas and is maintained at zero, and (3) the film is free from water.[19]

$$C(x,t) = C_0 - \frac{C_0 x}{l} - \frac{2}{\pi}\sum_{n=1}^{\infty}\frac{C_0}{n}\sin\frac{n\pi x}{l}\exp\left(-\frac{Dn^2\pi^2 t}{l^2}\right) \tag{4}$$

where D is the diffusivity of water vapor in the film. The flux profiles are obtained from the Fick's first law by differentiating $C(x,t)$ for distance. The total amount of water vapor Q which passes through the film in time t can be calculated from integration of the flux at $x = l$

$$Q = A\int_{t=0}^{t} J(l,t)\,\mathrm{d}t = AlC_0\left(\frac{Dt}{l^2} - \frac{1}{6} - \frac{2}{\pi^2}\sum_{1}^{\infty}\frac{(-1)^n}{n^2}\exp\left(-\frac{Dn^2\pi^2 t}{l^2}\right)\right) \tag{5}$$

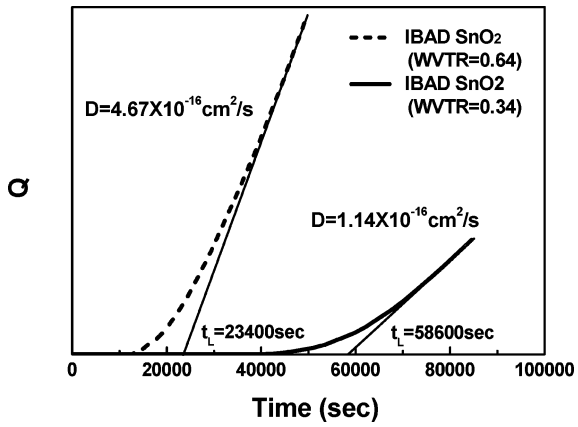

Figure 6. Total amount of water vapor permeated in time t through the IBAD SnO_2 films showing the WVTR values of 0.64 (- - -) and 0.34 g/m^2 day (—) at the steady state. t_L intercepted on the time axis is the time lag.

As time t increases, the flux through the film approaches the steady state, and then Q is expressed as

$$Q(t \rightarrow \infty) = \frac{ADC_0}{l}\left(t - \frac{l^2}{6D}\right) \quad (6)$$

The diffusivity D can be obtained from time lag t_L, intercepted on the time axis of the Q vs t plot

$$D = l^2/6t_L \quad (7)$$

The total WVTR values of 0.64 and 0.34 g/m^2 day at 37.8 °C, 100% RH for the SnO_2 films deposited at the ion beam current density of 30 and 35 μA/cm^2, respectively, on the PC substrates are small enough to be able to ignore the WVTR of 34 g/m^2 day for the PC substrate. Therefore, the permeation of water vapor through the bilayer of the IBAD SnO_2 films coated on the PC substrates can be considered identical to that through the single layer of the IBAD SnO_2 films. The permeation data of water vapor for the IBAD SnO_2 films showing the WVTR values of 0.64 and 0.34 g/m^2 day at the steady state are plotted in Figure 6, according to eq 6. The values of time lag, t_L = 23 400 and 58 600 s, are deduced, and the values of diffusivity, $D = 4.67 \times 10^{-16}$ and 1.14×10^{-16} cm^2/s, are calculated from eq 7 for the SnO_2 films deposited at the ion beam current density of 30 and 35 μA/cm^2, respectively.

In general, the diffusivity of water at 25 °C for the various polymers, such as poly(ethylene terephthalate) (PET), polyimide (PI), polyethersulfone (PES), and polycarbonate (PC), range from $\sim 10^{-8}$ to $\sim 10^{-9}$ cm^2/s.[20,21] With respect to the bulk oxide or the thin film oxide, there are little reports for the diffusivity of water estimated at low temperature (<50 °C). Roberts et al.[22] calculated the diffusivity of 2.9×10^{-16} cm^2/s for the bulk silica glass at 30 °C by extrapolating the high temperature (200 °C) data using Arrhenius equation. However, the diffusivity measured at high temperature is different from that measured at low temperature, because, at high-temperature, interaction between the OH groups and the permeating water vapor cannot contribute to activation energy for water vapor permeation, due to high thermal energy of water vapor. Graff et al.[23] deduced the diffusivity of the AlO_x film in a multilayer system consisting of a PET substrate, a first acrylic smoothing film, an AlO_x film, and a second acrylic smoothing film, from the measurement of the time lag. The AlO_x films were deposited by reactive magnetron sputtering and showed the diffusivity of 1.4×10^{-13} cm^2/s at 100% RH and 38 °C. Because the value of the diffusivity of water at low temperature has not been known for the SnO_2, our measured diffusivity for the SnO_2 films can be compared only with the diffusivity for the AlO_x films. The much lower diffusivity of 1.14×10^{-16} cm^2/s for the SnO_2 films deposited at the ion beam current density of 35 μA/cm^2 is related to the much higher activation energy of ~104 kJ/mol, compared to the activation energy of ~50 kJ/mol for the AlO_x films.[4] Therefore, we conclude that the SnO_2 films by IBAD effectively protect the permeation of water vapor by the low diffusivity due to the high activation energy, and when the SnO_2 films deposited at the ion beam current density of 45 μA/cm^2, showing the WVTR below 0.01 g/m^2 day, are used with the acrylic smoothing films in multilayer system, the number of layers required to satisfy the WVTR criterion of $<10^{-6}$ g/m^2 day at 100% RH and 25 °C in OLEDs can be significantly reduced.

4. Conclusion

Water chemically interacts with the oxide films and forms a multilayer consisting of the OH groups and the continuing adsorbed water vapor on the surface and the pore of the oxide films. Therefore, water vapor permeation through the oxide films is controlled by the oxide's polarizability and the packing density of the oxide films, because the oxide films with high polarizability and high packing density form the high OH groups on the pore, induce the strong interaction between the OH groups and water vapor, and then protect the permeation of water vapor.

We deposited the SnO_2 films of high polarizability by IBAD in order to increase the packing density with densely packed microstructure and compared the water vapor barrier properties with the SiO_x films of low polarizability. At all ion beam current densities, the SnO_2 films show lower WVTR than the SiO_x films, due to the higher polarizability. The SnO_2 films deposited at the ion beam current density of 35 μA/cm^2 show a much higher activation energy of ~104 kJ/mol, compared to the activation energy of ~66 kJ/mol for the SiO_x films, and the low diffusivity of 1.14×10^{-16} cm^2/s at 100% RH and 37.8 °C. At the ion beam current of 45 μA/cm^2, the SnO_2 films show the WVTR below the measurable limit of 0.01 g/m^2·day, whereas the SiO_x films show the higher WVTR of 0.6 g/m^2·day. Therefore, it is expected that, when the SnO_2 films deposited at the ion beam current density of 45 μA/cm^2 are combined with the acrylic smoothing films in multilayer system, the number of layers required to satisfy the WVTR criterion of $<10^{-6}$ g/m^2 day at 100% RH and 25 °C in OLEDs can be minimized.

References and Notes

(1) Weaver, M. S.; Michalski, L. A.; Rajan, K.; Rothman, M. A.; Silvernail, J. A.; Brown, J. J.; Burrows, P. E.; Graff, G. L.; Gross, M. E.; Martin, P. M.; Hall, M.; Mast, E.; Bonham, C.; Bennett, W.; Zumhoff, M. *Appl. Phys. Lett.* **2002**, *81*, 2929.

(2) Vogt, M.; Hauptmann, R. *Surf. Coat. Technol.* **1995**, *74*−*75*, 676.

(3) Erlat, A. G.; Henry, B. M.; Ingram, J. J.; Mountain, D. B.; McGuigan, A.; Howson, R. P.; Grovenor, C. R. M.; Briggs, G. A. D.; Tsukahara, Y. *Thin Solid Films* **2001**, *388*, 78.

(4) Erlat, A. G.; Henry, B. M.; Ingram, J. J.; Grovenor, C. R. M.; Briggs, G. A. D.; Chater, R. J.; Tsukahara, Y. *J. Phys. Chem. B* **2004**, *108*, 883.

(5) Henrich, V. E.; Cox, P. A. *The Surface Science of Metal Oxides*; Cambridge University Press: New York, 1996.

(6) Koo, W. H.; Jeong, S. M.; Choi, S. H.; Baik, H. K.; Lee, S. M.; Lee, S. J. *J. Phys. Chem. B* **2004**, *108*, 18884.

(7) Wu, C. C.; Lin, C. L.; Hsieh, P. Y.; Chiang, H. H. *Appl. Phys. Lett*. **2004**, *84*, 20.

(8) Tropsha, Y. G.; Harvey, N. G. *J. Phys. Chem. B* **1997**, *101*, 2259.

(9) Dimitrov, V.; Komatsu, T. *J. Solid State Chem*. **2003**, *163*, 100.

(10) Takeda, S.; Fukawa, M.; Hayashi, Y.; Matsumoto, K. *Thin Solid Films* **1999**, *339*, 220.

(11) Feng, A.; McCoy, J.; Munir, Z. A.; Cagliostro, D E. *J. Colloid Interface Sci*. **1996**, *180*, 276

(12) Yamazoe, N.; Fuchigami, J.; Kishikawa, M. *Surf. Sci.* **1979**, *86*, 335.

(13) Mohamed, S. H.; Kappertz, O.; Ngaruiya, J. M.; Niemeier, T.; Drese, R.; Detemple, R.; Wakkad, M. M.; Wuttig, *M. Phys. Status Solidi* **2004**, *201*, 90.

(14) Dreer, S.; Krismer, R.; Wilhartitz, P.; Friedbacher, G. *Thin Solid Films* **1999**, *354*, 43.

(15) Mohite, K. C.; Khollam, Y. B.; Mandale, A. B.; Patil, K. R.; Takwale, M. G. *Mater. Lett.* **2003**, *57*, 4170.

(16) Cuomo, J. J.; Rossnagel, S. M.; Kaufman, H. R. *Handbook Of Ion Beam Processing Technology*; Noyes Publications: New Jersey, 1989.

(17) Erlat, A. G.; Spontak, R. J.; Clarke, R. P.; Robinson, T. C.; Haaland, P. D.; Tropsha, Y.; Harvey, N. G.; Vogler, E. A. *J. Phys. Chem. B* **1999**, *103*, 6074.

(18) Raghu, P.; Yim, C.; Shadman, F.; Shero, E. *AIChE J.* **2004**, *50*, 1881.

(19) Crank, J. *The mathematics of diffusion*, 2nd ed.; Oxford University Press: London, 1975.

(20) Brandrup, J.; Immergut, E. H. *Polymer Handbook*, 3rd ed.; Wiley: New York, 1989.

(21) Métayer, M.; Labbé, M.; Marais, S.; Langevin, D.; Chappey, C.; Dreux, F.; Brainville, M.; Belliard, P. *Polym. Test.* **1999**, *18*, 533.

(22) Roberts, A. P.; Henry, B. M.; Sutton, A. P.; Grovenor, C. R. M.; Briggs, G. A. D.; Miyamoto, T.; Kano, M.; Tsukahara, Y.; Yanaka, M. *J. Membrane Sci.* **2002**, *1*, 5323.

(23) Graff, G. L.; Williford, R. E.; Burrows, P. E. *J. Appl. Phys.* **2004**, *96*, 1840.